Performance of Pt/Al-SBA-15 catalysts in hydroisomerization of *n*-dodecane

Cong Nie, Limin Huang, Dongyuan Zhao and Quanzhi Li *

Department of Chemistry, Fudan University, Shanghai 200433, PR China
E-mail: qzli@fudan.edu.cn

Received 18 July 2000; accepted 19 October 2000

A series of Al-SBA-15 materials with different Si/Al ratios have been prepared via a post-alumination procedure. The results show that Al species can be introduced into the SBA-15 framework. Only the medium acid sites can be observed on the Al-SBA-15 samples, and the number of acid sites decreases with the increase of the Si/Al ratio. The hydroisomerization activities of *n*-dodecane over 1% Pt/Al-SBA-15-n catalysts increase with the number of acid sites, and the largest isomers yield reaches to 51%. It suggests that the Al-SBA-15 material is a suitable acid component for bifunctional catalysts for hydroisomerization of long chain *n*-paraffins.

KEY WORDS: *n*-dodecane; hydroisomerization; SBA-15

1. Introduction

Catalytic dewaxing is believably the first industrial application of the shape-selectivity properties of zeolite catalyst [1]. A more attractive dewaxing procedure, isomerization dewaxing, through which *n*-paraffins are isomerizied to multibranched isoparaffins, avoids the yield loss resulted from the *n*-paraffins removal by cracking or solvent extraction [2,3].

Isomerization dewaxing catalysts are bifunctional, composed of both hydrogenation and acidic components. It has been reported that Al-containing mesoporous materials have a potential application in isomerization catalytic dewaxing due to their mild acidities. For example, bifunctional Pt/Al-MCM-41 catalysts have been used to isomerize *n*-hexane and *n*-hexadecane [4,5]. Marler et al. [6] combined the hydrocracking and hydroisomerization processes in order to convert wax feed to high viscocisity index lubricants. Pt/MCM-41 catalysts were involved in this process, which produced less waxy branched paraffins. Girgis et al. [5] used the bifunctional Pt/MCM-41 catalysts to investigate the reaction pathways and kinetics of *n*-hexadecane hydroisomerization and hydrocracking. However, the lack of hydrothermal stability of mesoporous MCM-41 materials limits their further applications in the field of catalysis.

A recently discovered pure silica phase, designated as SBA-15, has a 31 to 64 Å thick siliceous wall that imparts greater hydrothermal stability in boiling water to SBA-15 in comparison with MCM-41 materials [7]. Moreover, in our recent study, SBA-15 could maintain its mesostructure under steaming (100% H_2O) treatment at 800 °C for 8 h, whereas the mesostructure of MCM-41 totally collapsed under the same condition just for 2 h. Thus, highly-ordered mesoporous silica SBA-15 has great potential for use in the catalytic field. Unfortunately, as the pure silica SBA-15 is synthesized in strong acid media (2 M HCl solution), incorporation of framework aluminum into SBA-15 by direct synthesis seems impossible because most aluminum sources dissolve in strong acids. Previous studies have shown that aluminum can be effectively incorporated into siliceous MCM-41 material via various post-synthesis procedures by grafting aluminum onto MCM-41 wall surfaces with anhydrous $AlCl_3$ [8] or aluminum isopropoxide in nonaqueous solution [9], or with sodium aluminate in aqueous solution [10] followed by calcination. More recently, several papers have reported the alumination of SBA-15 molecular sieves [11,12]. However, the acidity and catalytic properties of Al-SBA-15 supported noble metal catalysts for the hydroisomerization of normal paraffins have not been reported yet so far.

In this paper, a series of Al-SBA-15 catalysts with different Si/Al ratios have been prepared via post-synthesis procedure by reacting SBA-15 with aluminum isopropoxide in dry hexane, and their acidic properties have been measured by NH_3-TPD and FT-IR techniques. The hydroisomerization of *n*-dodecane was studied over Pt/Al-SBA-15 catalysts with different Si/Al ratios. Moreover, the influence of the balance between acid and hydrogenating function was discussed.

2. Experimental

2.1. Catalysts

A detailed synthesis procedure for mesoporous SBA-15 has been reported elsewhere [7]. In a typical synthesis in this work, 2 g of amphiphilic triblock copolymer, poly(ethylene oxide)–poly(propylene oxide)–poly(ethylene oxide) (average molecular weight 5800, from Aldrich) was dispersed in

* To whom correspondence should be addressed.

1011-372X/01/0100-0117$19.50/0

15 g of water and 60 g of 2 M HCl solution at 40 °C while stirring, followed by the addition of 4.25 g of tetraethylorthosilicate (from Aldrich) to the homogeneous solution with stirring. This gel mixture was continuously stirred at 40 °C for 24 h, and finally crystallized in a Teflon-lined autoclave at 100 °C for 2 days. After cooling to room temperature the solid product was filtered and dried at room temperature in air. The calcination was carried out in static air at 550 °C for 6 h to decompose the triblock copolymer to obtain a white powder (SBA-15).

Aluminum-containing materials, Al-SBA-15, were prepared via post-synthesis route according to the following procedure. 0.5 g calcined SBA-15 was dispersed in 50 ml dry hexane containing various amounts of aluminum isopropoxide. The resulting mixture was stirred at room temperature for 12 h, and the powder was filtered, washed with dry hexane and dried at room temperature in air. The solid powder was calcined in static air at 550 °C for 5 h. These materials are denoted as Al-SBA-15-n, (n = 1, 2, 3 and 4). Pt loading catalysts, Pt/Al-SBA-15-n (Pt 1 wt%), were prepared by incipient wetness impregnation of Al-SBA-15-n with the aqueous solution of chloroplatinic acid (pH = 9, adjusted by $NH_3{\cdot}H_2O$). This was followed by evaporation, drying at 120 °C for 12 h, and calcination at 500 °C for 8 h in air.

2.2. Characterization

Powder X-ray diffraction (XRD) patterns were recorded on a Rigaku D/MAX-II A X-ray powder diffractometer, which employed Ni-filtered Cu Kα radiation and was operated at 40 kV and 20 mA.

The nitrogen adsorption and desorption isotherms at 77 K were measured using a Micromeritics ASAP 2000 system. The pore structural data were analyzed by the BJH (Barrett–Joyner–Halenda) method using the Halsey equation for multilayer thickness. The pore size distribution curve came from the analysis of the desorption branch of the isotherm.

NH_3-TPD was performed on 100 mg of the catalyst with helium (40 ml/min) as the carrier gas and a thermoconductor as the detector. The catalyst was pretreated *in situ* by heating in helium flow at 550 °C for 1 h and saturated with ammonia at 120 °C, then the NH_3-TPD test was started with a heating rate of 15 °C /min.

H_2–O_2 titration experiments were carried out in a pulsed system with Ar as the carrier gas and a thermoconductor as the detector. H_2 (or O_2) was injected into the catalyst bed through a six-port valve with a sample loop. All the gases used were properly purified before using.

IR spectra of pyridine adsorption were obtained on a Nicolet 5SXC FTIR spectrometer. The self-supporting wafers of about 5 mg/cm^2 were first evacuated *in situ* in an IR cell at 350 °C for 4 h, and the spectra were recorded after cooling to room temperature. Pyridine was then admitted and after equilibrium the samples were degassed at 120, 180, 240 and 300 °C, respectively, and the corresponding spectra were recorded.

^{27}Al MAS NMR spectra were recorded at room temperature on a Bruker MSL-300 spectrometer with a resonance frequency of 78.21 MHz. The magnetic field was 7.05 T. The spin rate of the sample was 4.0 kHz and the number of scans was 4000–5000. The pulse lengths were adjusted to 4.6 μs with repetition time to 500 ms. The sweep width was 29477 Hz. $AlCl_3{\cdot}6H_2O$ was used as a reference.

2.3. Catalytic test

The catalytic conversion of *n*-dodecane was carried out in a pulse microreactor at a pressure of 2.2 bar and a hydrogen flow rate of 40 ml/min. The catalyst (40 mg) with the particle size of 0.28–0.45 mm loaded in a fix-bed reactor was pretreated *in situ* by heating at 400 °C for 2 h in hydrogen followed by the injection of 1 μl of reactant into the catalyst bed. Reactants and products were analyzed on line by a gas chromatograph, with a flame-ionization detector, and equipped with a capillary OV-101 column (50 m length, 0.25 mm i.d.).

3. Results and discussion

3.1. Physical properties of catalysts

XRD patterns of SBA-15 and aluminated SBA-15-n products are shown in figure 1. All samples show well-resolved patterns with a prominent diffraction peak (100), and two additional diffraction peaks indexed to (110) and

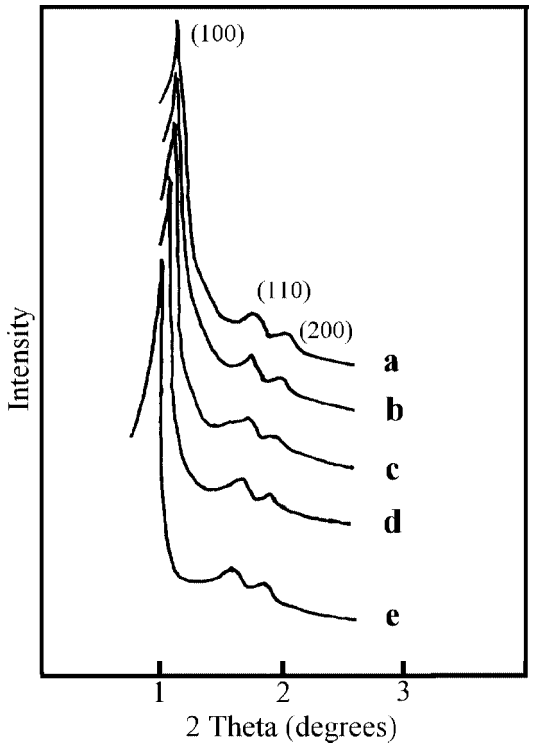

Figure 1. XRD patterns of calcined Al-SBA-15-n: (a) Al-SBA-15-1, (b) Al-SBA-15-2, (c) Al-SBA-15-3, (d) Al-SBA-15-4 and (e) SBA-15.

(200) reflections, which match well with the pattern reported for SBA-15 [7], indicating all Al-SBA-15 products prepared by post-alumination have well-ordered hexagonal mesostructures. However, the diffraction peaks of Al-SBA-15-n samples all shift to higher 2θ degrees compared with SBA-15. This may result from the constriction of their frameworks with further calcination during the alumination procedure. Moreover, the XRD lines of Pt/Al-SBA-15-n, as given in figure 2, also show three typical peaks for hexagonal mesoporous SBA-15, although the peak intensities show a little decrease. The result indicates that the loading of Pt species via an incipient wetness impregnation does not deteriorate the hexagonal mesostructures of the Al-SBA-15-n materials.

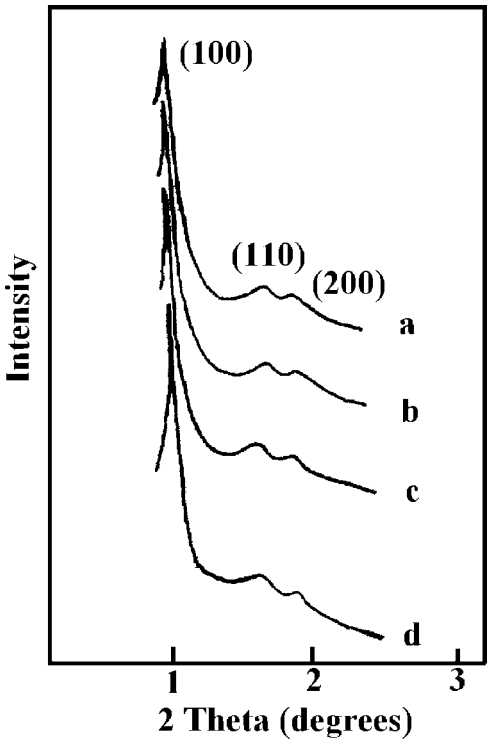

Figure 2. XRD patterns of calcined Pt/Al-SBA-15-n: (a) Pt/Al-SBA-15-1, (b) Pt/Al-SBA-15-2, (c) Pt/Al-SBA-15-3 and (d) Pt/Al-SBA-15-4.

Table 1 summarizes the properties of mesoporous Al-SBA-15-n and Pt-loaded Al-SBA-15-n samples. It reveals the successful synthesis of Al-SBA-15-n samples with very different Si/Al ratios from 8 to 60, which can be controlled by changing the amount of aluminum isopropoxide in dry hexane during the post-synthesized procedure. However, aluminum content has little influence on textual properties of Al-SBA-15-n materials. The surface area and average pore diameter of Al-SBA-15-n materials are similar to the parent SBA-15, indicating that post-alumination procedure does not destroy the mesostructure of SBA-15. Table 1 also reveals that Pt dispersion on the catalysts is unalterable (around 40%) with the different Si/Al ratios of Al-SBA-15-n samples.

3.2. ^{27}Al MAS NMR

Figure 3 shows the ^{27}Al MAS NMR spectra of Al-SBA-15-n samples prepared by post-alumination. All spectra give two resolved lines at 53 and 0 ppm. The line at 53 ppm can be assigned to aluminum in a tetrahedral environment (AlO_4 structural unit, Al(tet)), in which aluminum is covalently bound to four framework Si atoms via oxygen bridges. The chemical shift at 0 ppm can be assigned to octahedral extraframework aluminum (AlO_6 structural unit, Al(oct)). According to the presence of AlO_4 structural units in the framework of Al-SBA-15-n samples, it is definite that the aluminum is successfully incorporated into the siliceous SBA-15 framework during the alumination procedure with aluminum isopropoxide. Like siliceous MCM-41 materials [14], the siliceous SBA-15 also possesses a large number of silanol groups on the wall surfaces, which are suggested to serve as active sites for aluminum grafting. On the other hand, the formation of AlO_4 structural units may result from the incorporation of aluminum into the structural defects of the siliceous SBA-15 and react with the neighboring silanol groups. Table 1 shows that the values of Al(tet)/[Al(tet) +

Table 1
Physical properties of Al-SBA-15 and Pt/Al-SBA-15 catalysts.

Catalyst	S_{BET} (m^2/g)	APD[a] (Å)	Si/Al[b]	Al(tet)/ [Al(tet) + Al(oct)][c]	Framework Si/Al(tet)	D[d] (%)	n_{Pt}/n_A[e]
SBA-15	829	56					
Al-SBA-15-1	642	58	7.5	0.72	10.4	–	
Al-SBA-15-2	664	58	15.5	0.81	19.3	–	
Al-SBA-15-3	707	57	33.4	0.88	37.9	–	
Al-SBA-15-4	728	57	60.2	0.90	67.1	–	
Pt/Al-SBA-15-1			–	–	–	43	0.26
Pt/Al-SBA-15-2			–	–	–	46	0.35
Pt/Al-SBA-15-3			–	–	–	39	0.42
Pt/Al-SBA-15-4			–	–	–	41	0.69

[a] APD = average pore diameter (determined using BJH analysis).
[b] From chemical analysis.
[c] Calculated from ^{27}Al MAS NMR spectra assuming that the relative content of aluminum is proportional to the intensity of the ^{27}Al MAS NMR lines.
[d] Platinum dispersion from H_2–O_2 titration.
[e] n_{Pt} is the number of accessible platinum atoms; n_A is the number of Brønsted acid sites calculated from Py-IR results.

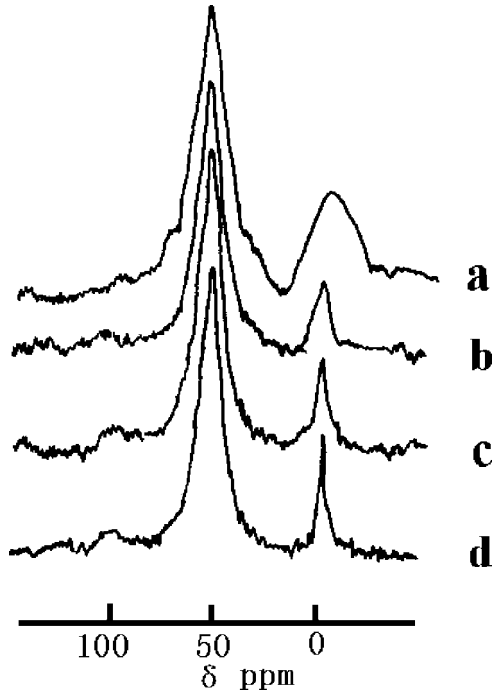

Figure 3. ^{27}Al MAS NMR spectra of calcined Al-SBA-15-n prepared by post-synthesis procedure in dry hexane: (a) Al-SBA-15-1, (b) Al-SBA-15-2, (c) Al-SBA-15-3 and (d) Al-SBA-15-4.

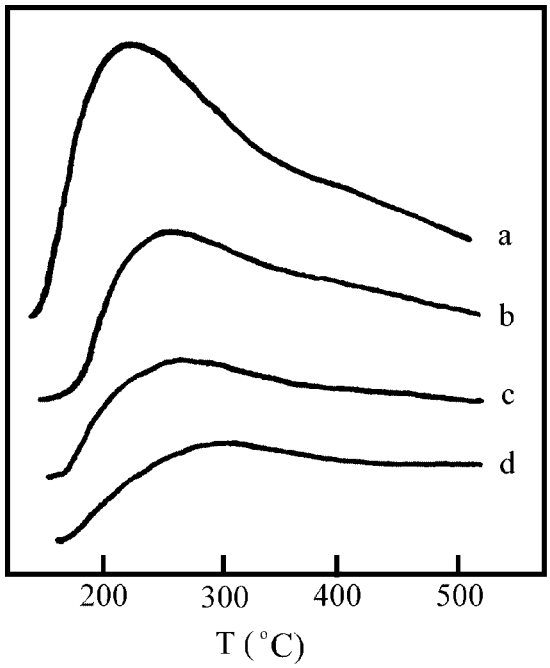

Figure 4. NH_3-TPD curves of Al-SBA-15-n: (a) Al-SBA-15-1, (b) Al-SBA-15-2, (c) Al-SBA-15-3 and (d) Al-SBA-15-4.

Al(oct)] increase with the Si/Al ratio, indicating that the efficiency of aluminum incorporation decreases with the increase of the concentration of aluminum species during the alumination procedure.

3.3. Acid properties of catalysts

NH_3-TPD results of Al-SBA-15-n and Pt-loaded Al-SBA-15-n catalysts (Pt 1 wt%) are given in figures 4 and 5, respectively. All Al-SBA-15 samples with different aluminum contents show only lower temperature peaks at about 270 °C related to mild acid sites, while the desorption peak of ammonia is too broadened to be detected at a temperature higher than 300 °C corresponding to strong acid sites (see figure 4). Moreover, the total acid numbers of Al-SBA-15 samples decrease remarkably with the increase of Si/Al ratio (see table 2). These phenomena are similar to the previous reports for Al-MCM-41 [15,16]. As seen in figure 5, Pt/Al-SBA-15-n catalysts show the same acid features as the corresponding Pt-free Al-SBA-15-n samples. However, the total acid number of the Pt-loading sample is less than that of its parent support alone (table 2). The decrease of the acid sites may result from the coverage of Pt species on some acid sites.

IR spectra of pyridine adsorption on Al-SBA-15-n and Pt/Al-SBA-15-n catalysts at variable temperatures are shown in figures 6 and 7, respectively. Table 2 lists the acid distribution of each catalyst quantitatively calculated from the IR spectra of pyridine desorption at 120, 180 and 240 °C, respectively. From figures 6 and 7, both Brønsted (band at 1540 cm^{-1}) and Lewis (band at 1450 cm^{-1}) acid sites

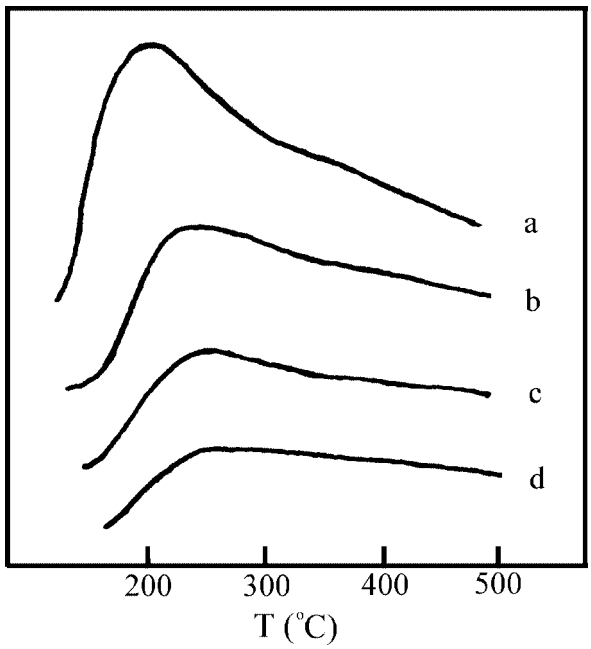

Figure 5. NH_3-TPD curves of Pt/Al-SBA-15-n: (a) Pt/Al-SBA-15-1, (b) Pt/Al-SBA-15-2, (c) Pt/Al-SBA-15-3 and (d) Pt/Al-SBA-15-4.

can be observed on Al-SBA-15-n and Pt/Al-SBA-15-n catalysts. It can be seen from the IR spectra and table 2 that the number of Brønsted acid sites is lower than that of Lewis acid sites on all Pt-free and Pt-loading samples. The deficit of Brønsted acid sites for these samples is probably caused by dehydroxylation during the calcination, in which the Brønsted acid sites are stepwise transformed to Lewis acid sites. According to table 2, the number of total acid sites (represented by n_{B+L} at 120 °C) decrease with the in-

Table 2
The number of acid sites on Al-SBA-15 and Pt/Al-SBA-15 catalysts.[a]

Catalyst	n_B[b] ($\times 10^{19}$/g)			n_L[b] ($\times 10^{19}$/g)			n_{B+L} ($\times 10^{19}$/g)			n_O[c]
	120 °C	180 °C	240 °C	120 °C	180 °C	240 °C	120 °C	180 °C	240 °C	($\times 10^{19}$/g)
Al-SBA-15-1	5.07	3.83	1.96	12.7	7.06	5.84	17.8	10.9	7.80	24.1
Al-SBA-15-2	4.04	2.96	1.55	9.46	6.81	5.24	13.5	9.77	6.79	20.0
Al-SBA-15-3	2.84	1.85	0.97	7.04	5.65	4.54	9.88	7.50	5.51	14.2
Al-SBA-15-4	1.82	1.54	0.43	5.77	4.01	3.46	7.59	5.55	3.89	7.5
Pt/Al-SBA-15-1	4.55	3.27	1.38	9.95	6.70	5.30	14.5	9.97	6.68	22.3
Pt/Al-SBA-15-2	3.47	2.36	1.08	7.66	6.36	4.67	11.1	8.72	5.75	17.8
Pt/Al-SBA-15-3	2.16	1.27	0.82	6.63	5.68	3.07	8.79	6.95	3.89	11.4
Pt/Al-SBA-15-4	1.42	1.01	0.36	5.24	3.40	2.81	6.66	4.41	3.17	6.3

[a] Represented by pyridine adsorption number per g catalyst after being degassed at 120, 180 and 240 °C, respectively.
[b] From extinction coefficient by Emeis [21].
[c] Ammonia number desorbed out of the sample during NH_3-TPD test.

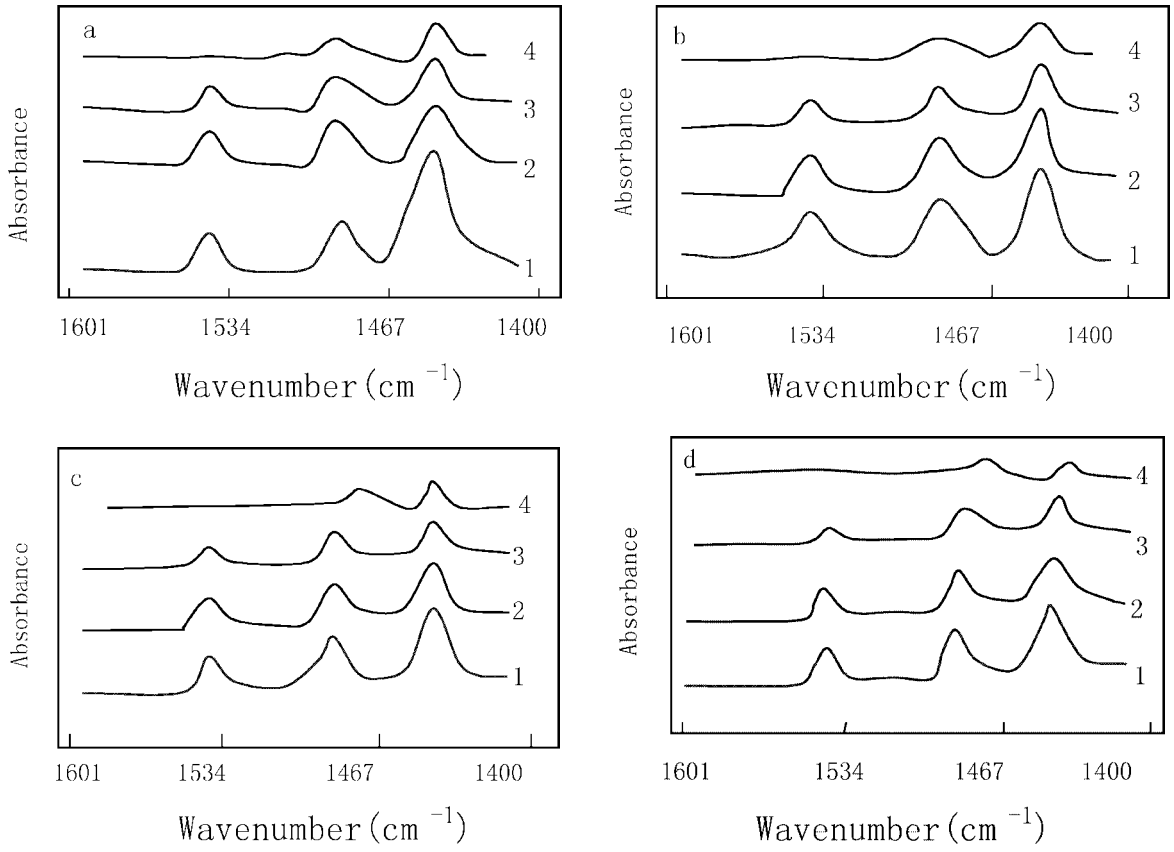

Figure 6. IR spectra of pyridine adsorbed on Al-SBA-15-n after being degassed at variable temperature: (a) Al-SBA-15-1, (b) Al-SBA-15-2, (c) Al-SBA-15-3 and (d) Al-SBA-15-4; (1) 120, (2) 180, (3) 240 and (4) 300 °C.

crease of Si/Al ratio for all samples, which is in agreement with the result from NH_3-TPD test. Moreover, after pyridine desorption at 300 °C, all of the pyridine associated with protons has been desorbed, indicating that the Brønsted acid sites on Al-SBA-15 are of medium strength. For Al-SBA-15 with different Si/Al ratios, although they possess different numbers of Brønsted acid sites, their acid strengths are almost the same. These phenomena are in agreement with those in the above NH_3-TPD spectra. The acidities of Pt/Al-SBA-15-n catalysts are similar to those of their counterpart.

3.4. Catalytic performance of catalysts

The conversion of *n*-dodecane measured over Pt/Al-SBA-15-n (Pt 1 wt%) in the reaction temperature range of 275–375 °C is shown in figure 8. It clearly illustrates that the conversion of *n*-dodecane over the samples increases with the increase of the temperature. Figure 8 also reveals that the conversion of *n*-dodecane varies obviously with the change of acid sites. The less the Si/Al ratio is, the more the number of acid sites is, and the larger the conversion of *n*-dodecane

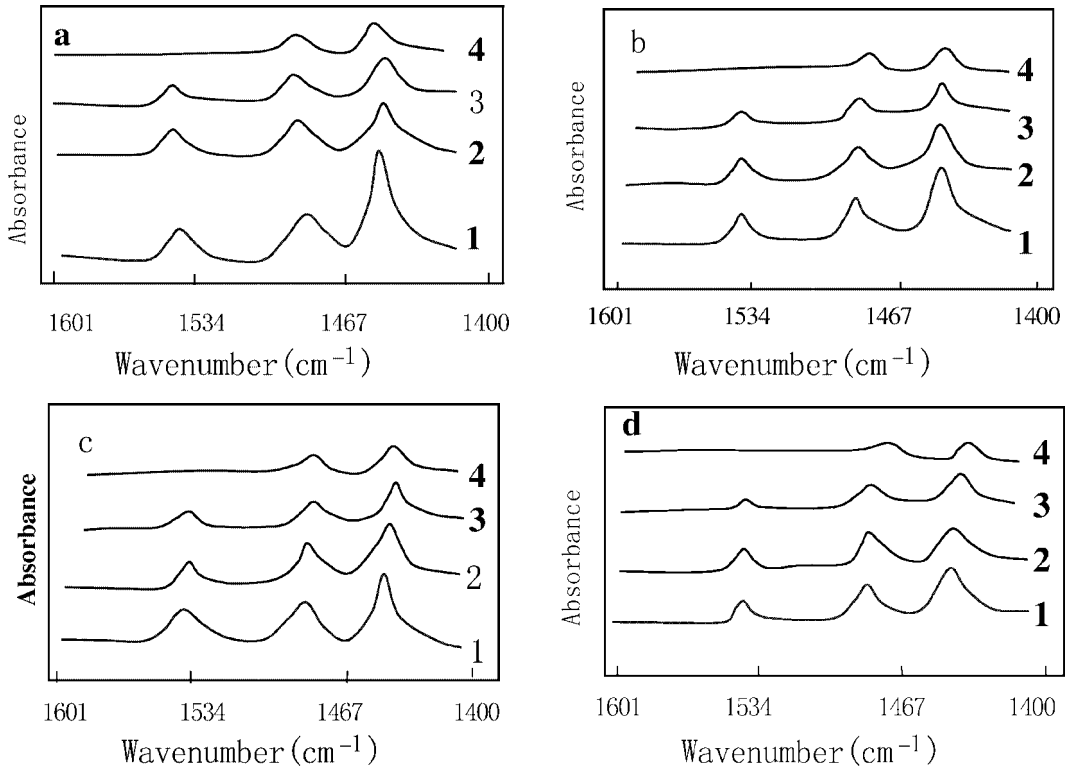

Figure 7. IR spectra of pyridine adsorbed on Pt/Al-SBA-15-n after being degassed at variable temperature: (a) Pt/Al-SBA-15-1, (b) Pt/Al-SBA-15-2, (c) Pt/Al-SBA-15-3 and (d) Pt/Al-SBA-15-4; (1) 120, (2) 180, (3) 240 and (4) 300 °C.

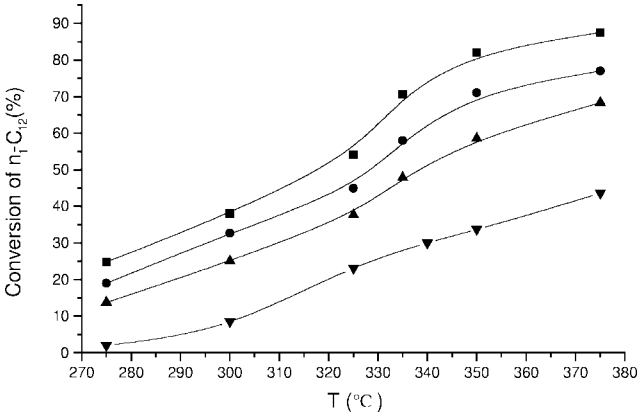

Figure 8. Conversion of *n*-dodecane over Pt/Al-SBA-15-n catalysts as a function of the reaction temperature: (■) Pt/Al-SBA-15-1, (●) Pt/Al-SBA-15-2, (▲) Pt/Al-SBA-15-3 and (▼) Pt/Al-SBA-15-4.

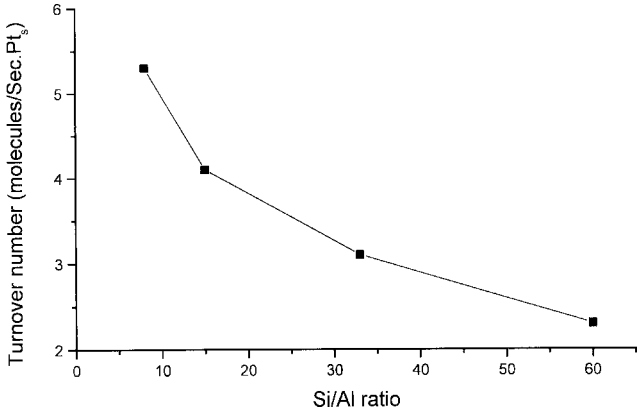

Figure 9. Effect of the Si/Al ratio of the support of Pt/Al-SBA-15 catalysts on the turnover number of *n*-dodecane at reaction temperature of 335 °C.

is. However, one might think that this difference of conversions could arise from the different Pt dispersions in this catalyst system. Thus, the turnover numbers, the numbers of *n*-dodecane molecules converted per surface metal site per second, for Pt/Al-SBA-15-n catalysts are calculated. These are shown as a function of the Si/Al ratio of the support of Pt/Al-SBA-15-n catalysts in figure 9. It is clear for *n*-dodecane that very different turnover numbers are observed depending on the Si/Al ratio of the catalyst support. Similar to the conversion trend in figure 8, figure 9 illustrates that the conversion increases with the decrease of the Si/Al ratio of the catalyst support. For comparison, the catalytic performance of Pt/SBA-15 catalyst is investigated under the same reaction conditions. It shows no hydroisomerization and hydrocracking activity.

Plots of the yields of *n*-dodecane isomers and cracking products against total *n*-dodecane conversion over Pt/Al-SBA-15-n catalysts are shown in figure 10 (a)–(d). As seen in figure 10, the isomers yield is a unique function of the total conversion for all four catalysts. At low conversions *n*-dodecane is hydroisomerized without hydrocracking reactions occurring. With the increase of *n*-dodecane conversion, isomerization conversion passes through a maximum, owing to the consumption of isomerized products in consecutive hydrocracking reactions. This observation may rule out

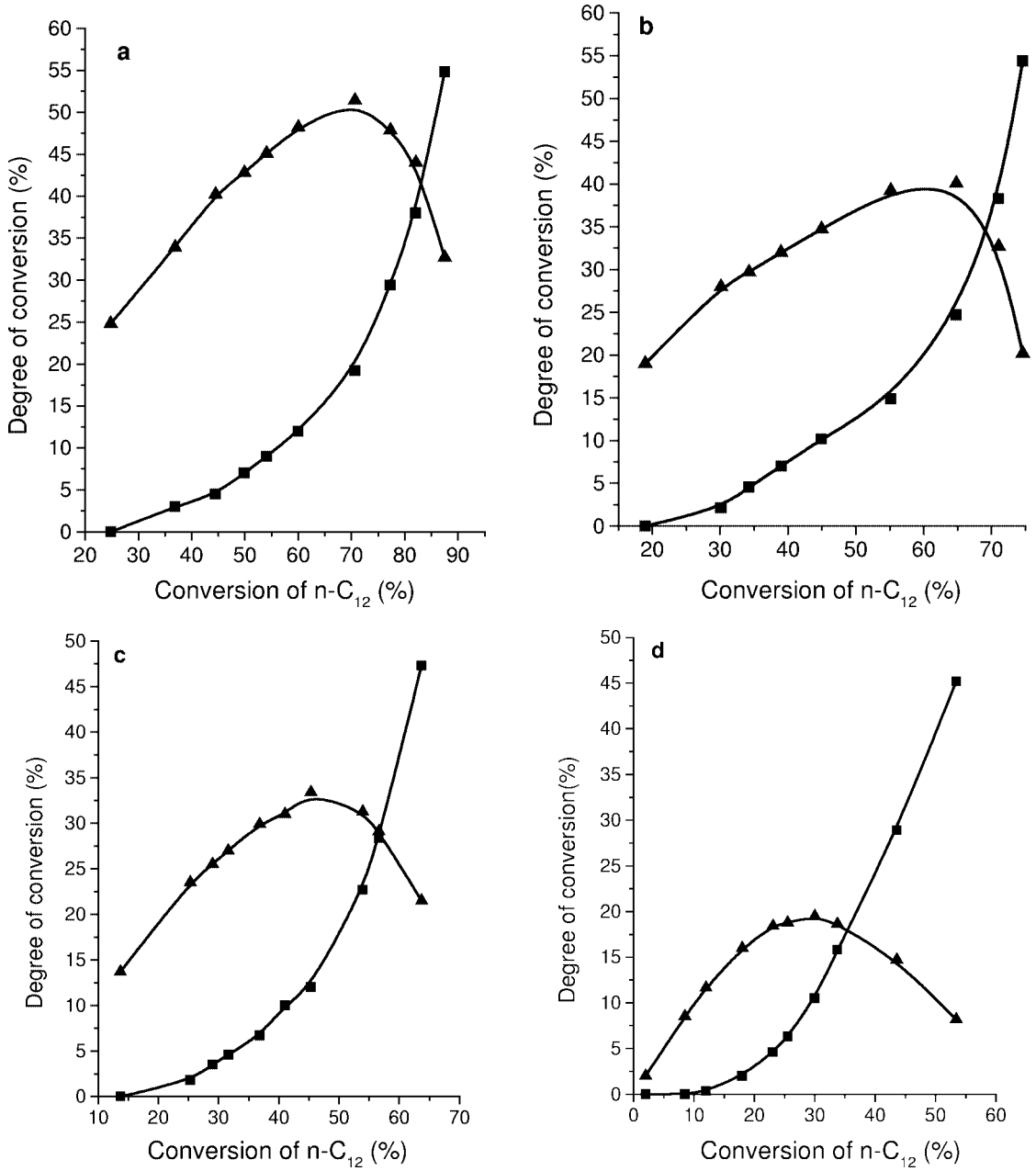

Figure 10. Products distribution as a function of the total conversion of *n*-dodecane over Pt/Al-SBA-15-n catalysts: (a) Pt/Al-SBA-15-1, (b) Pt/Al-SBA-15-2, (c) Pt/Al-SBA-15-3 and (d) Pt/Al-SBA-15-4.

the possibility of a direct cracking of the *n*-dodecane without reactant structural rearrangement [17]. At the reaction temperature of 335 °C, the largest isomers yields over Pt/Al-SBA-15-n (n = 1, 2, 3 and 4) catalysts amount to 51, 40, 31 and 20%, respectively. The larger the number of Brønsted acid sites is, the more the isomers yield is. It suggests that the Brønsted acid number has a great influence on the catalytic properties of Pt/Al-SBA-15-n catalysts for the hydroisomerization of *n*-dodecane. In order to describe the influence of the acid component in the bifunctional catalysts more clearly, we plotted the largest isomers yields of Pt/Al-SBA-15-n catalysts against the number of Brønsted acid sites on these catalysts (see figure 11). It reveals that the largest isomers yields of Pt/Al-SBA-15-n catalysts are proportional to the number of Brønsted acid sites, indicating that the hydroisomerization activities of Pt/Al-SBA-15-n catalysts depend on the number of Brønsted acid sites of those catalysts. Moreover, it can be suggested that for the post-aluminated Al-SBA-15 materials, almost all aluminum atoms related to the generation of acidity are distributed on the wall surface of the framework, thus providing more acid sites than Al-MCM-41 with the same Si/Al ratio which is synthesized directly. For instance, with the same Si/Al ratio of 20 (gel mixture), Al-MCM-41material has a Brønsted acid number of only 2.0×10^{19}/g while Al-SBA-15 material has a Brønsted acid number of 2.8×10^{19}/g. Since the hydroisomerization activity greatly depends on the Brønsted acid number, it is reasonable that the Pt/Al-SBA-15 catalyst

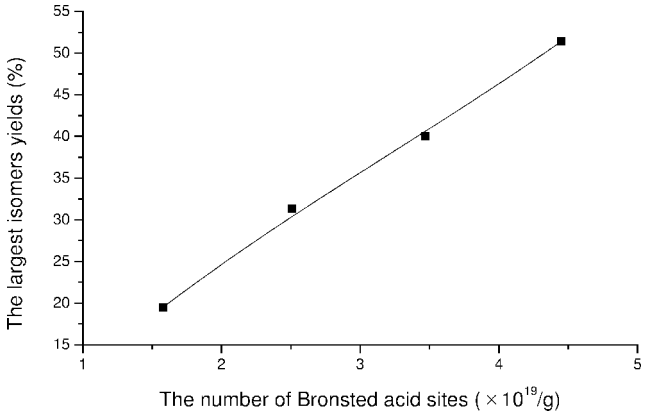

Figure 11. The largest isomers yields of n-dodecane over Pt/Al-SBA-15-n catalysts as a function of the number of Brønsted acid sites n-dodecane.

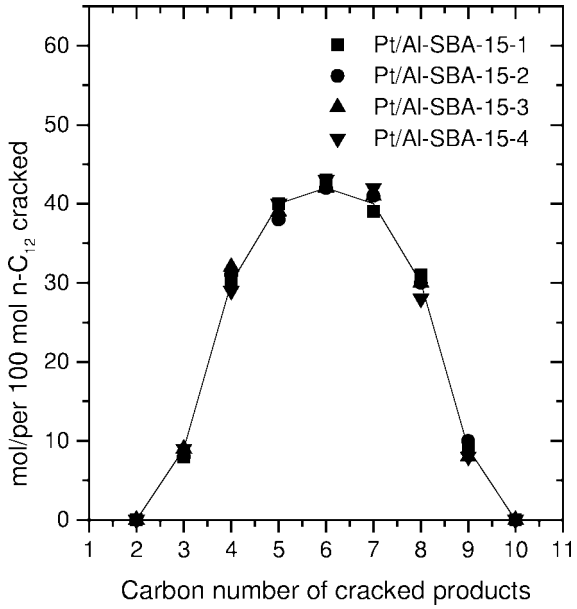

Figure 12. Selectivities for the cracked products of n-dodecane as a function of carbon number of these products.

has the largest isomers yield of 33.4%, which is higher than that of 25.7% [18] for Pt/Al-MCM-41 (Pt 1 wt%) under the same reaction conditions. In addition, because of its higher thermal and hydrothermal stability, the Pt/Al-SBA-15 catalyst has more potential application in industry compared with the Pt/Al-MCM-41 catalyst.

The distributions of cracked products in terms of carbon number are presented in figure 12. For Pt/Al-SBA-15-n catalysts, C_1 and C_2 as well as C_{10} and C_{11} are absent, suggesting that no hydrogenolysis of n-dodecane on the acid sites occurs. The distributions are symmetrical, indicating no secondary cracking occurs [19]. In addition, all catalysts lead to the similar distribution.

The ratio of monobranched to multibranched dodecane isomers (M/B) as a function of the total conversion is given in figure 13. It is clear that the product distribution of isomers is a function of the total conversion, and the ratio M/B decreases with the increase of the total conversion. This is in line with the observation by Weitkamp et al. [17] and Jacobs et al. [20], who pointed out that the monobranched isomers are formed with a branching mechanism via protonated cyclopropanes (PCP intermediates), whereas multibranched structures are formed in consecutive reactions from the monobranched isomers of the products. Concerning the result (given in figure 10) that a direct cracking of the n-dodecane without reactant structural rearrangement is impossible and no secondary cracking occurs (given in figure 12), we can draw a conclusion that for Pt/Al-SBA-15-n catalysts, the n-dodecane should transfer as the following scheme: $n\text{-}C_{12} \rightleftharpoons M \rightleftharpoons B \rightarrow C$.

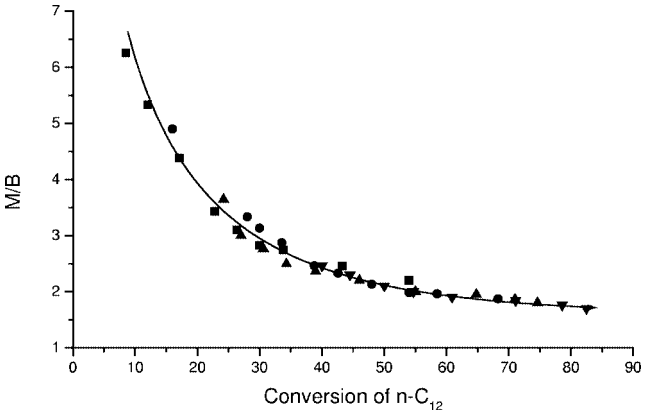

Figure 13. The ratio of monobranched to multibranched dodecane isomers (M/B) as a function of the total conversion of n-dodecane over Pt/Al-SBA-15-n catalysts: (■) Pt/Al-SBA-15-4, (●) Pt/Al-SBA-15-3, (▲) Pt/Al-SBA-15-2 and (▼) Pt/Al-SBA-15-1.

For a bifunctional catalyst, besides the acid function, the balance between acid and hydrogenating functions, which is characterized by the ratio of the number of hydrogenating sites to the number of Brønsted acid sites (n_{Pt}/n_A), also has a great influence on the catalytic property of the catalyst. Alvarez et al. [21] have reported this influence on the transformation of n-decane over Pt/HY catalysts, where he pointed out that for bifunctional catalyst, when the value of n_{Pt}/n_A is higher than a certain value (which is different with the catalytic system), it will be in the proper balance between acid and hydrogenating functions. And the number of acid sites encountered by the olefinic intermediates is such that only one transformation can occur before hydrogenation. Therefore this catalyst can be considered as ideal. For an ideal catalyst, the activity per acid sites is maximal and the maximum activity should be proportional to the number of acid sites. Moreover, for an ideal catalyst, whatever the catalyst is, the M/B ratio should be constant at the same conversion of the reactant. For Pt/Al-SBA-15-n catalysts with different n_{Pt}/n_A from 0.26 to 0.69, the largest isomers yields are proportional to the numbers of Brønsted acid sites of those catalyts, and the M/B ratios depend on the conversion of n-C_{12} only. Based on these facts, Pt/Al-SBA-15-n catalysts can be considered as ideal bifunctonal catalysts. In other words, the ideal situation occurs when the number of Brønsted acid sites which may be encountered by the olefinic intermediates during their diffusion between

two metallic sites is lower than 4 ($n_{Pt}/n_A \geqslant 0.26$) for Pt/Al-SBA-15-n catalysts.

In addition, the isomerization conversions of *n*-octane and *n*-decane are investigated over the Pt/Al-SBA-15-1 catalyst for comparison. For *n*-octane with shorter alkyl chain length, even at a high reaction temperature of 375 °C, the conversion is only 37% and the largest isomers yield is 20%. With increasing the alkyl chain length, the largest isomers yield can reach 34% at a reaction temperature of 355 °C for *n*-decane. For *n*-dodecane, the largest isomers yield amounts to 51% at a reaction temperature of 335 °C. Therefore, we draw the conclusion that because of its medium strength, Al-SBA-15 is a suitable acid component for a bifunctional catalyst in the hydroisomeriaztion of long chain paraffins.

4. Conclusion

Al-SBA-15 mesoporous material prepared via post-alumination is found to be a suitable acid component for the bifunctional Pt/Al-SBA-15 catalyst in the hydroisomerization of long chain *n*-dodecane, due to its medium strength. The largest isomers yield of *n*-dodecane reaches 51% at a reaction temperature of 335 °C for Pt/Al-SBA-15 with Si/Al ratio of 8. With the same Si/Al ratio, the largest isomers yield for Pt/Al-SBA-15 is higher than that for Pt/Al-MCM-41. A proper balance between acid and hydrogenating functions is also found for the Pt/Al-SBA-15 catalyst. The transition scheme of *n*-dodecane is $n\text{-}C_{12} \rightleftharpoons M \rightleftharpoons B \rightarrow C$.

Acknowledgement

Financial support from the National Natural Science Foundation of China (Project 29733070) is gratefully acknowledged.

References

[1] K.W. Smith, W.C. Starr and N.Y. Chen, Oil Gas J. (1980) 75.
[2] S.J. Miller, US Patent 4 689 138 (1987).
[3] R. Parton, L. Uytterhoeven, J.A. Martens and P.A. Jacobs, Appl. Catal. 76 (1991) 131.
[4] K.J. Del Rossi, G.H. Hatzikos and A. Huss, Jr., US Patent 5 256 277 (1993).
[5] M.J. Girgis and Y.P. Tsao, Ind. Eng. Chem. Res. 35 (1996) 386.
[6] D.O. Marler and D.N. Mazzone, US Patent 5 288 395 (1994).
[7] D. Zhao, J. Feng, Q. Huo, N. Melosh, G.H. Fredrickson, B.F. Chmelka and G.D. Stucky, Science 279 (1998) 548.
[8] R. Ryoo, S. Jun and J.M. Kim, J. Chem. Soc. Chem. Commun. (1997) 2225.
[9] R. Mokaya and W. Jones, J. Chem. Soc. Chem. Commun. (1997) 2185.
[10] H. Hamdan, S. Endud, H. He, M.N.M. Muhid and J. Klinowski, J. Chem. Soc. Faraday Trans. 92 (1996) 2331.
[11] Z. Luan, M. Hartmann, D. Zhao, W. Zhou and L. Kevan, Chem. Mater. 11 (1999) 1621.
[12] M. Chen, Z. Wang, K. Sakurai, F. Kumata, T. Saito, T. Komatsu and T. Yashima, Chem. Lett. (1999) 131.
[13] R. Ryoo and J.M. Kim, J. Chem. Soc. Chem. Commun. (1995) 711.
[14] W. Kolodziejski, A. Corma, M.T. Navarro and J. Perez-Pariente, J. Solid State NMR 2 (1993) 253.
[15] X.Y. Chen, L.M. Huang, G.Z. Ding and Q.Z. Li, Catal. Lett. 44 (1997) 123.
[16] A. Corma, V. Fornes, M.T. Navarro and J. Perez-Pariente, J. Catal. 148 (1994) 569.
[17] J. Weitkamp, Ind. Eng. Chem. Res. Dev. 21 (1982) 550.
[18] L.M. Huang, W. Xu, C. Nie and Q.Z. Li, unpublished results.
[19] M. Steijns, G. Froment, P. Jacobs, J. Uytterhoeven and J. Weitkamp, Ind. Eng. Chem. Res. Dev. 20 (1981) 654.
[20] J.A. Martens and P.A. Jacobs, in: *Theoretical Aspects of Heterogenerous Catalysis*, ed. J.B. Moffat (Van Nostrand Reinhold, New York, 1990) p. 52.
[21] F. Alvarez, F.R. Ribeiro, G. Perot, C. Thomazeau and M. Guisnet, J. Catal. 162 (1996) 179.
[22] C.A. Emeis, J. Catal. 141 (1993) 347.